Magnetically driven winds from differentially rotating neutron stars and X-ray afterglows of SGRBs

RICCARDO CIOLFI

in collaboration with:

Daniel Siegel and Luciano Rezzolla

Siegel, Ciolfi and Rezzolla, ApJ 785, L6 2014
(arXiv:1401.4544)

Gamma-Ray Bursts in the Multi-messenger Era
IPGP - Paris, June 19th 2014

INTRODUCTION

leading model of short gamma-ray bursts (SGRBs)

central engine is a black hole surrounded by hot thick torus
⟶ end result of a binary neutron star (BNS) merger

Paczynski 1986 , Eichler et al. 1989
Narayan et al. 1992 , ...

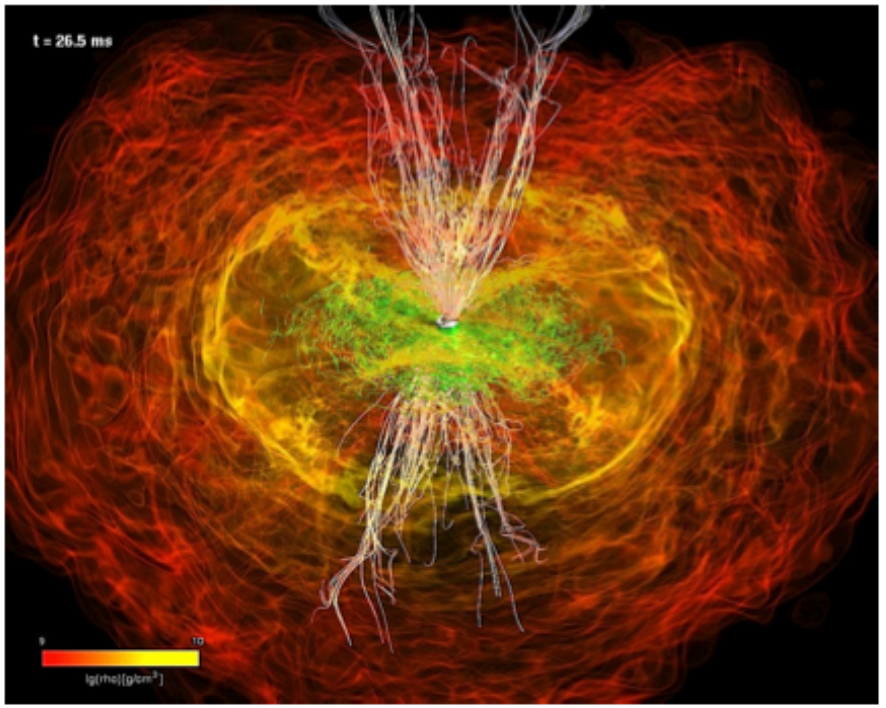

Rezzolla et al 2011

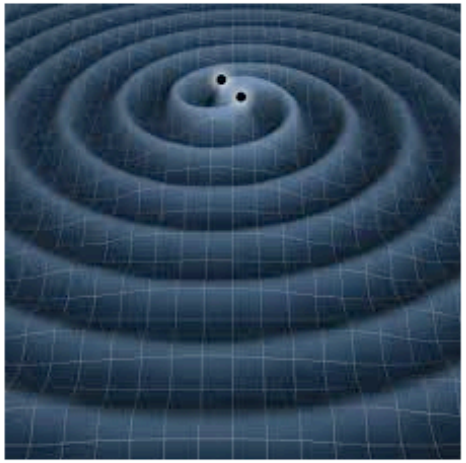

BNSs are also among the most promising sources of gravitational waves

likely of rate ~40/yr for Adv LIGO and Virgo
possibility of combined GW-EM detection !

X-RAY AFTERGLOWS OF SGRBs

- SWIFT revealed that many SGRBs are accompanied by long-duration $(10 - 10^4\ \mathrm{s})$ and high-luminosity $(10^{46} - 10^{51}\ \mathrm{erg/s})$ X-ray afterglows
- total energy can be higher than the SGRB itself
- hardly produced by BH-torus system - they suggest ongoing energy injection from a long-lived NS

MAGNETAR MODEL

Zhang & Meszaros 2001

X-ray emission ⟶ spindown of a uniformly rotating NS with a strong surface magnetic field

$$\gtrsim 10^{14} - 10^{15}\,\mathrm{G}$$

dipole spindown

$$L_{\rm sd}(t) \sim B^2 R^6 \Omega_0^4 \left(1 + \frac{t}{t_{\rm sd}}\right)^{-2}$$

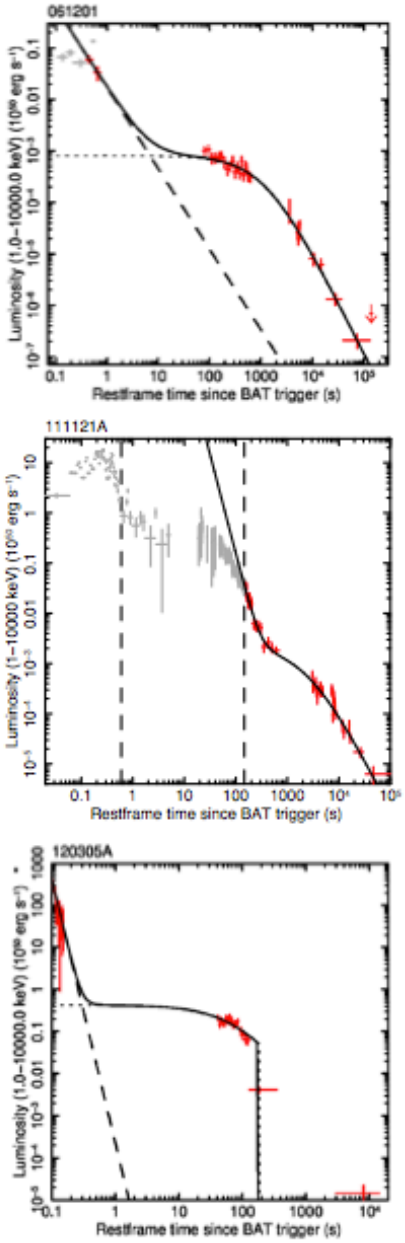

Gompertz et al. 2013

Rowlinson et al. 2013

X-RAY AFTERGLOWS OF SGRBs

- SWIFT revealed that many SGRBs are accompanied by long-duration $(10 - 10^4\ \mathrm{s})$ and high-luminosity $(10^{46} - 10^{51}\ \mathrm{erg/s})$ X-ray afterglows
- total energy can be higher than the SGRB itself
- hardly produced by BH-torus system - they suggest ongoing energy injection from a long-lived NS

MAGNETAR MODEL

Zhang & Meszaros 2001

X-ray emission ⟶ spindown of a uniformly rotating NS with a strong surface magnetic field

$$\gtrsim 10^{14} - 10^{15}\,\mathrm{G}$$

dipole spindown

$$L_{\rm sd}(t) \sim B^2 R^6 \Omega_0^4 \left(1 + \frac{t}{t_{\rm sd}}\right)^{-2}$$

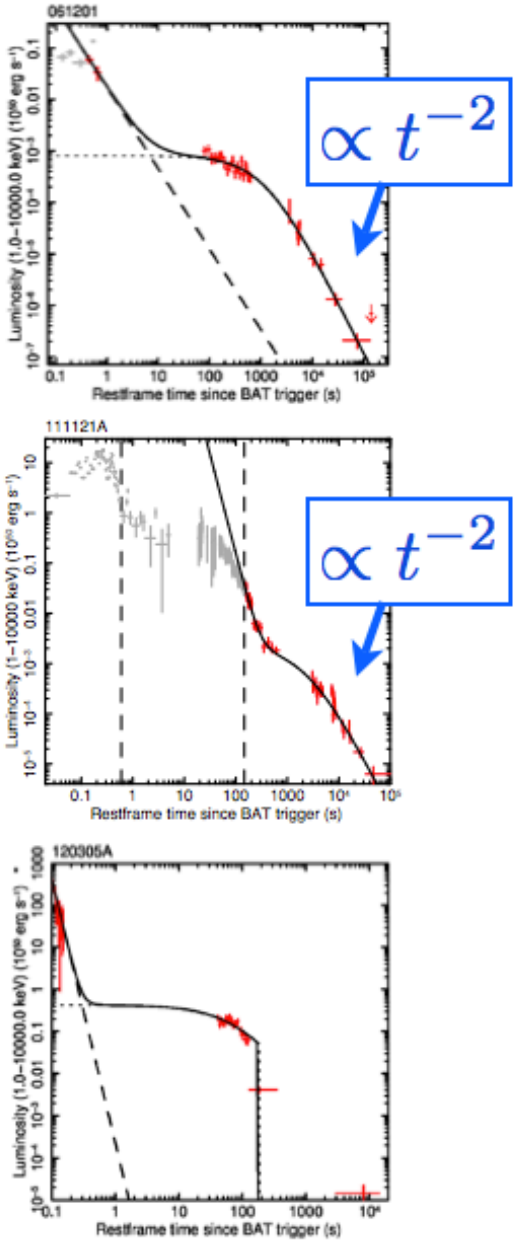

Gompertz et al. 2013

Rowlinson et al. 2013

PRODUCT OF BNS MERGERS

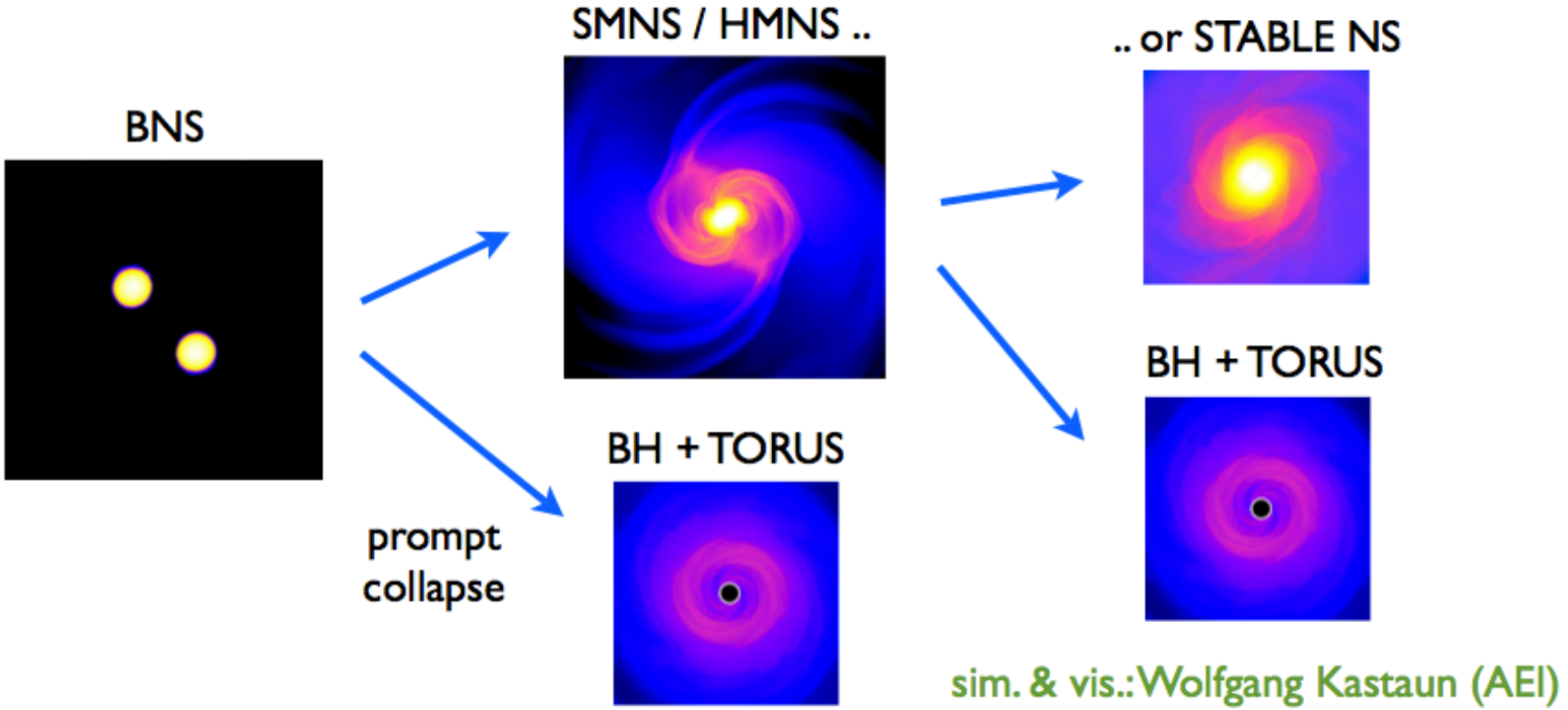

LONG-LIVED NS IS A LIKELY OUTCOME OF THE MERGER

- observation of $\sim 2\ \mathrm{M}_\odot$ NSs — Demorest et al. 2010, Antoniadis et al. 2013
- progenitor masses peak around $1.3 - 1.4\ \mathrm{M}_\odot$ → BMP mass likely $< 2.5\ \mathrm{M}_\odot$ — Belczynski et al. 2010
- stable NS obtained in GR BNS merger simulations — Giacomazzo & Perna 2013

PRODUCT OF BNS MERGERS

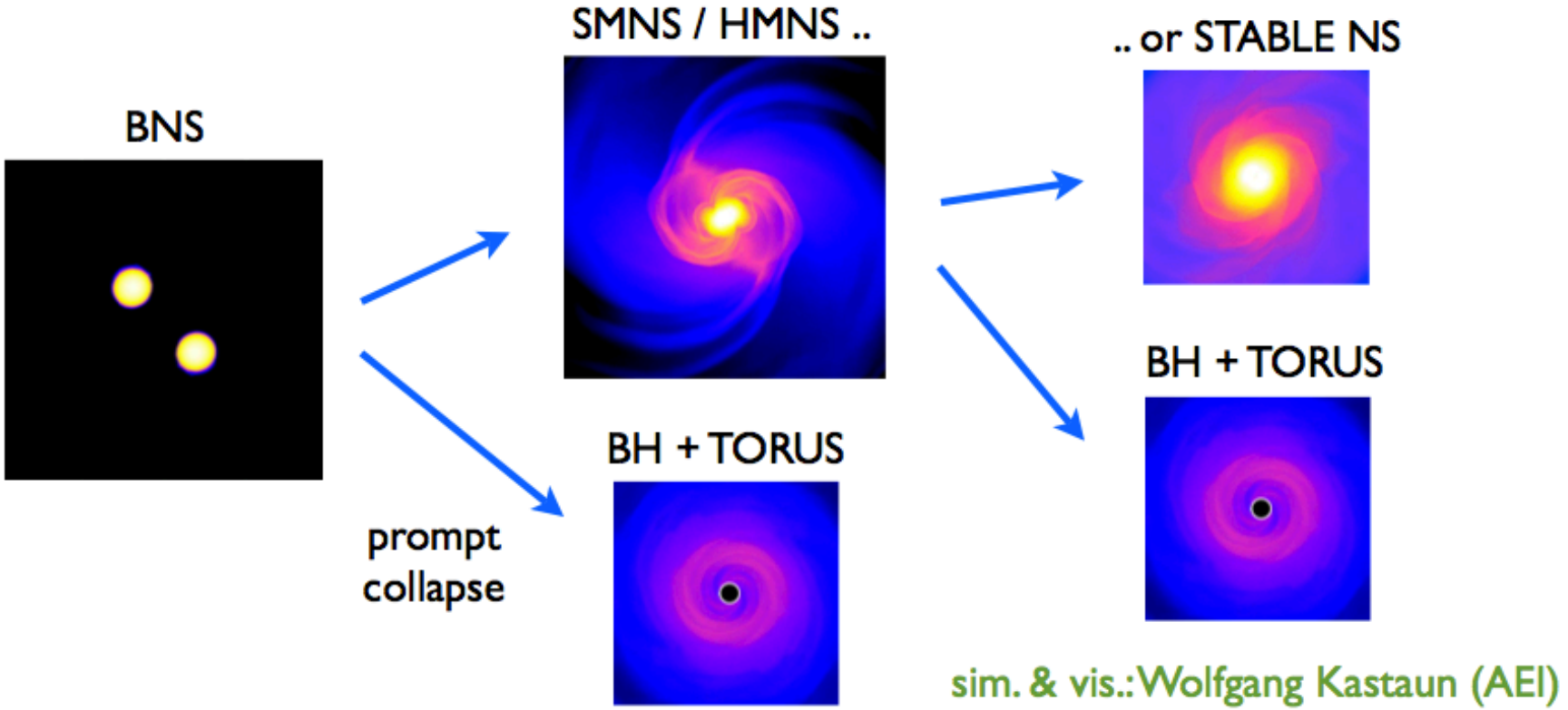

LONG-LIVED NS IS A LIKELY OUTCOME OF THE MERGER

newly-born NS is DIFFERENTIALLY ROTATING

→ EARLY DYNAMICS DIFFERS FROM SIMPLE DIPOLE SPINDOWN !

GRMHD EVOLUTION OF HMNSs

long-lived NS scenario: open issues

- early properties of merger product
- prompt SGRB emission
- early X-ray afterglows ('extended emission')
- mass ejection, effect on EM emission
- ...

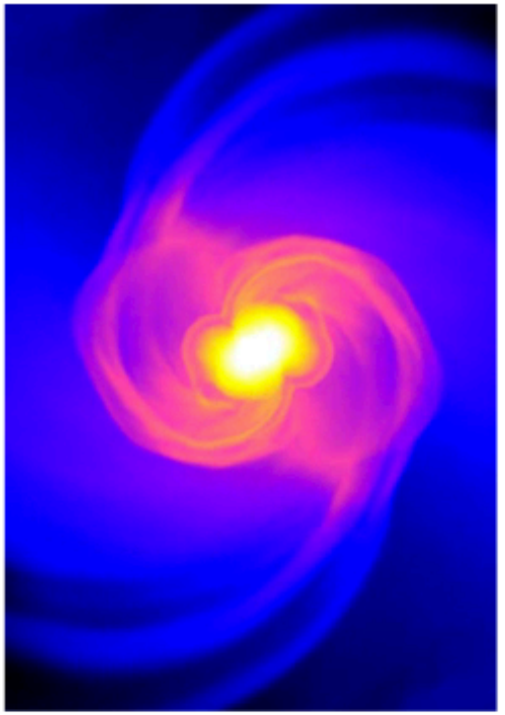

we study the early evolution of a magnetized HMNS via 3D MHD simulations in General Relativity

a powerful emission mechanism emerges, driven by differential rotation..

HMNS EVOLUTION

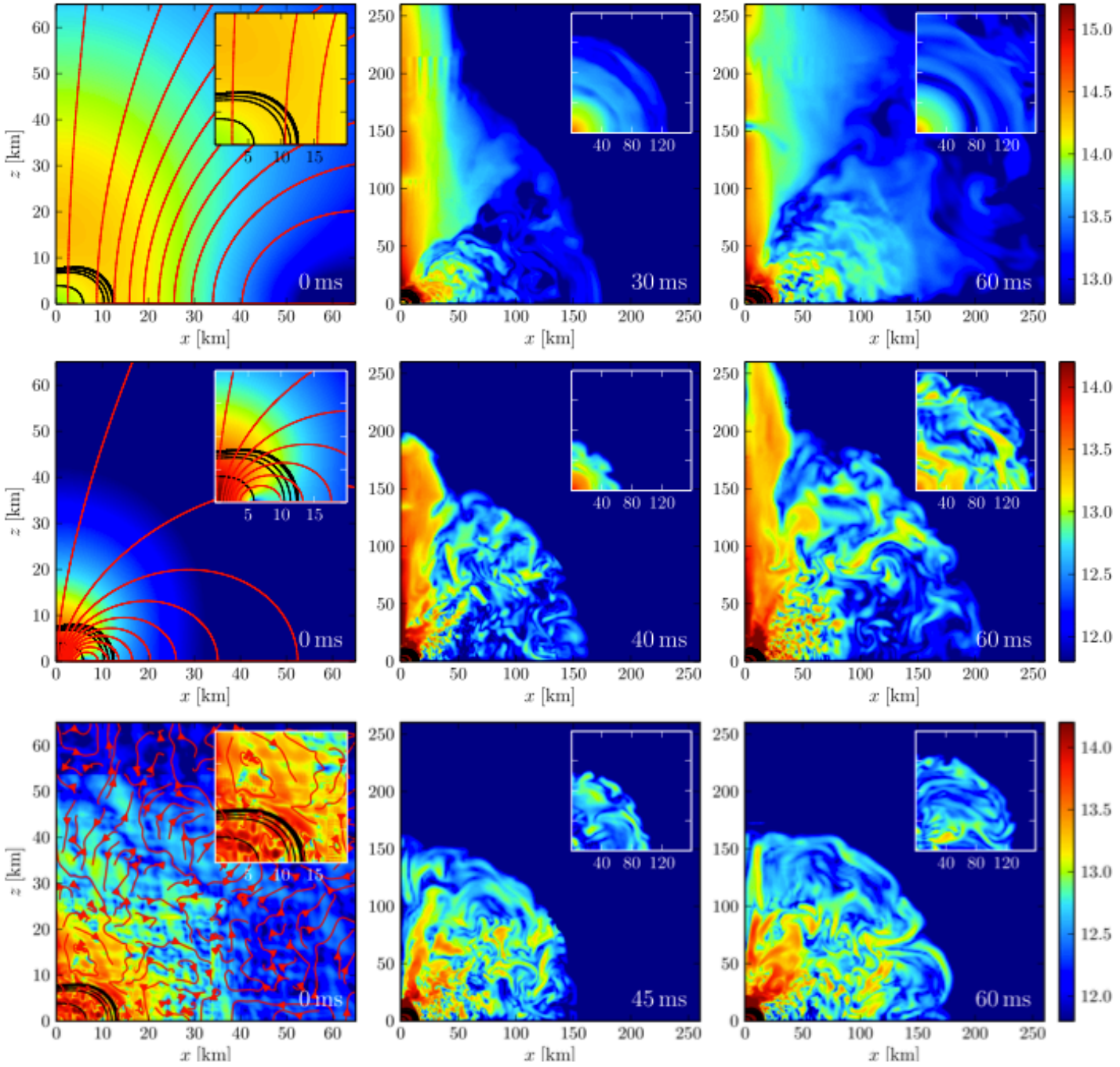

60 ms evolution
for 3 geometries

dipole 60
dipole 6
random

differential rotation
powers baryon-loaded
and magnetized outflow

for all MF geometries
the outflow has an
isotropic component

collimation depends
strongly on MF
geometry

BARYON-LOADED WIND

- rest-mass density of the wind $\rho \sim 10^8\ \mathrm{g/cm^3}$
- ejection speed $v \lesssim 0.1\ \mathrm{c}$
- mass loss rate $\dot{M} \sim 10^{-3}\ \mathrm{M_\odot/s}$
- mostly isotropic!

rand

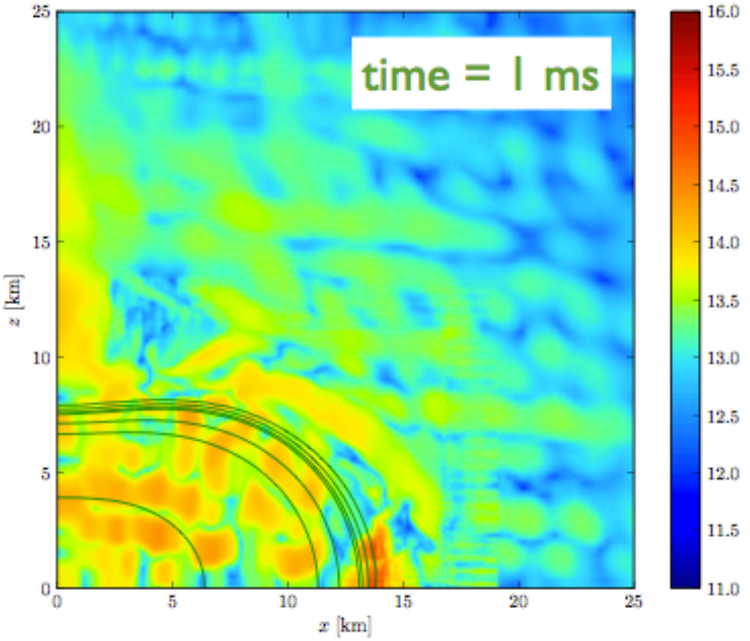

rest-mass density evolution ↓

dipole 60

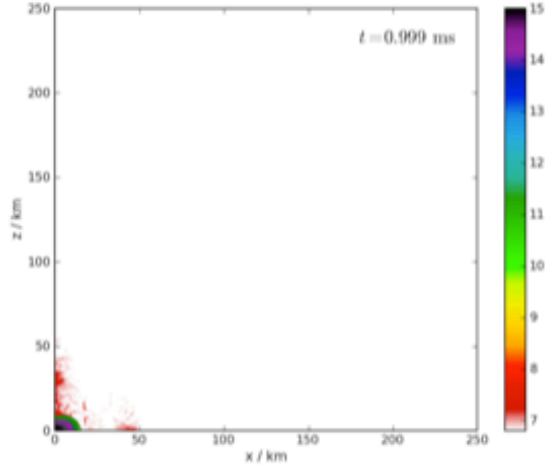

dipole 6

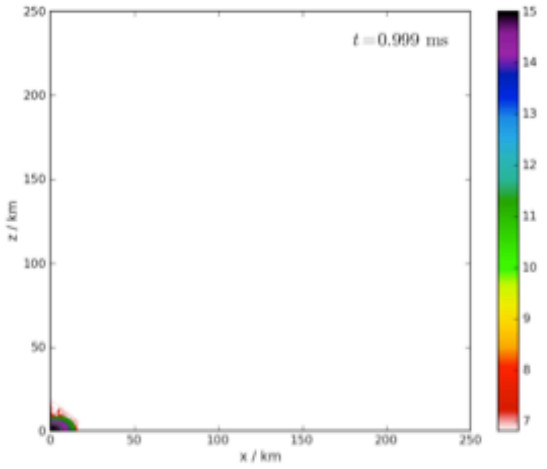

rand

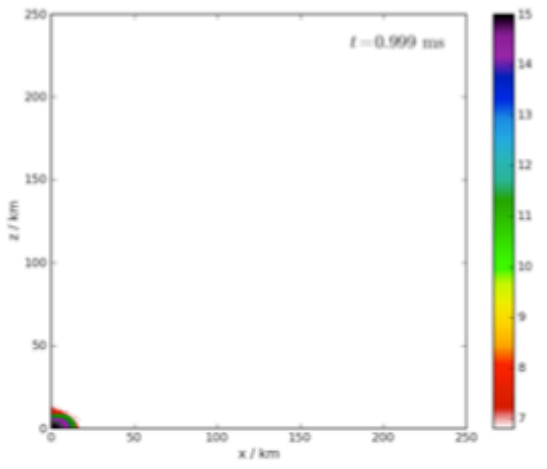

BARYON-LOADED WIND

- rest-mass density of the wind $\rho \sim 10^8\ \mathrm{g/cm^3}$
- ejection speed $v \lesssim 0.1\ \mathrm{c}$
- mass loss rate $\dot{M} \sim 10^{-3}\ \mathrm{M_\odot/s}$
- mostly isotropic!

rand

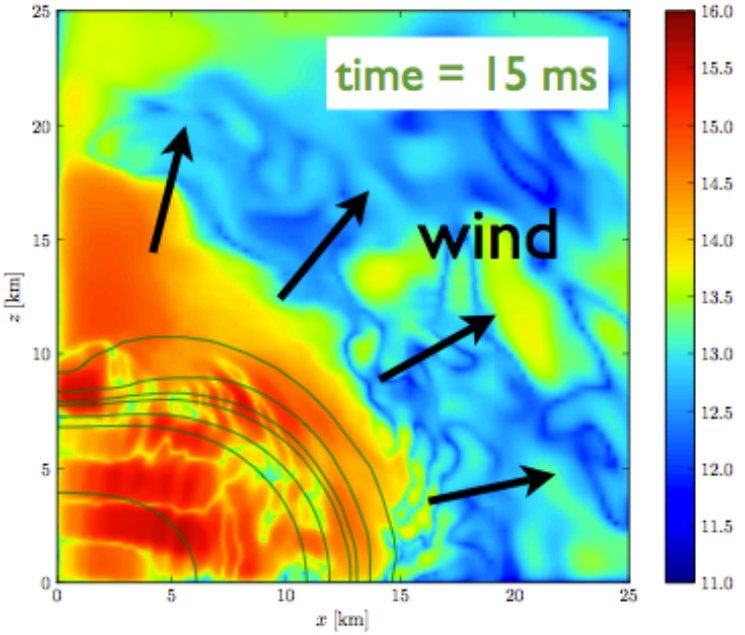

rest-mass density evolution ↓

dipole 60

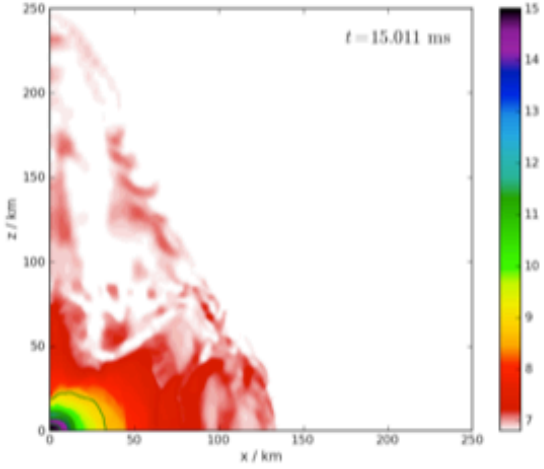

dipole 6

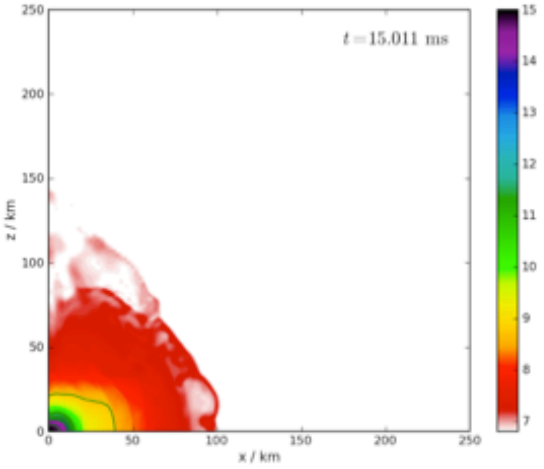

rand

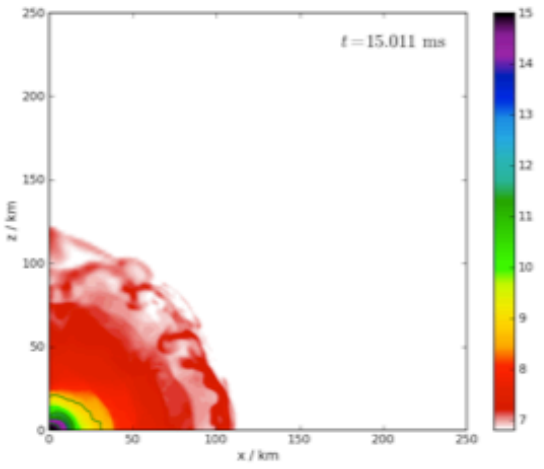

BARYON-LOADED WIND

- rest-mass density of the wind $\rho \sim 10^8\ \mathrm{g/cm^3}$
- ejection speed $v \lesssim 0.1\ \mathrm{c}$
- mass loss rate $\dot{M} \sim 10^{-3}\ \mathrm{M_\odot/s}$
- mostly isotropic!

rand

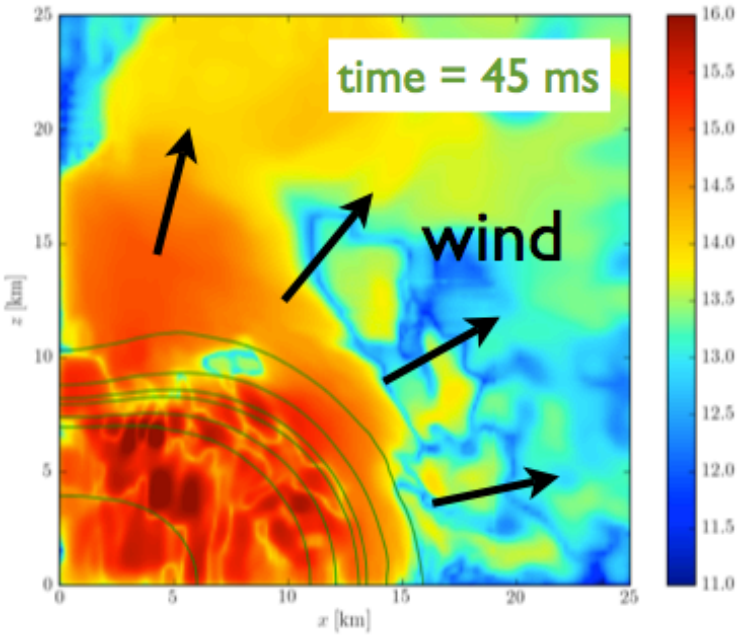

rest-mass density evolution ↓

dipole 60

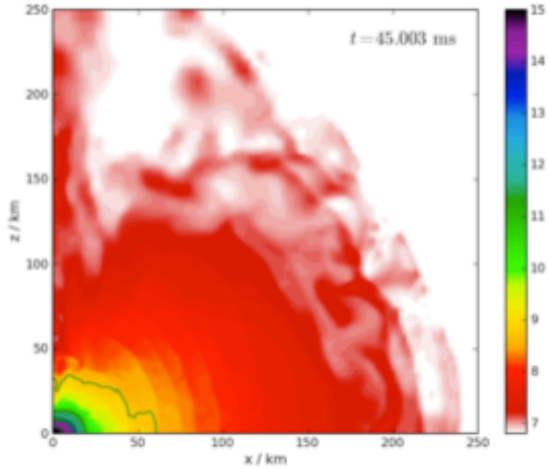

dipole 6

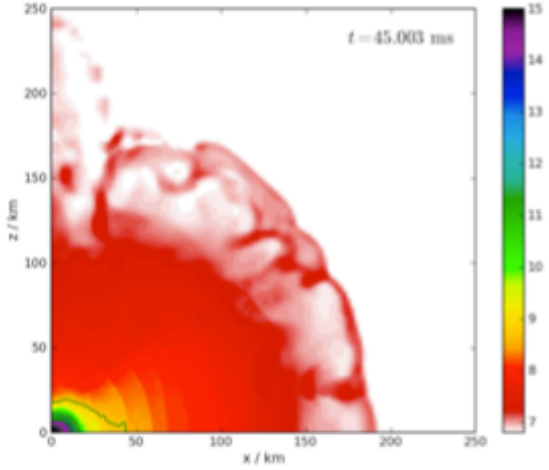

rand

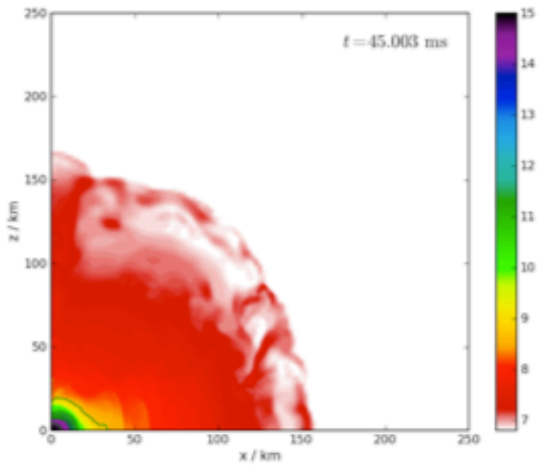

EM LUMINOSITY

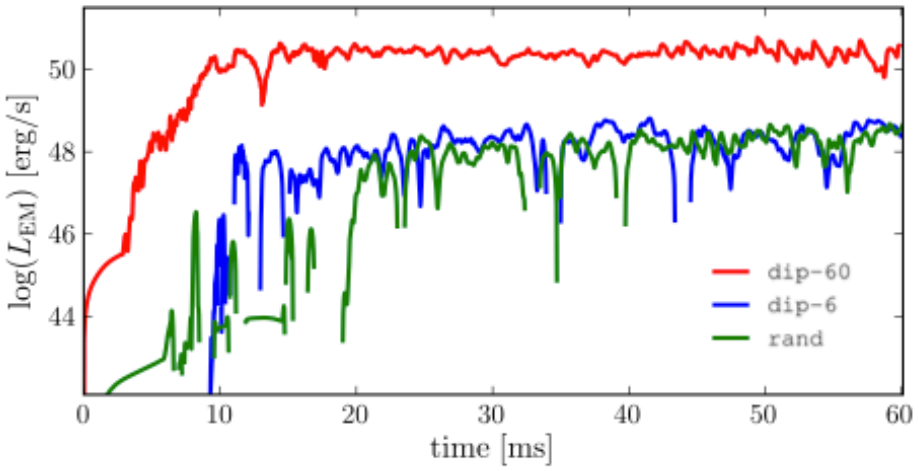

$$L_{\rm EM} \simeq 10^{48} \chi \left(\frac{B_0}{10^{14}\,{\rm G}}\right)^2 \left(\frac{R_e}{10^6\,{\rm cm}}\right)^3 \left(\frac{P}{10^{-4}\,{\rm s}}\right)^{-1} {\rm erg\,s^{-1}}$$

scaling different from dipole spindown $L_{\rm sd} \propto B^2 R^6 \Omega^4$

results reproduced with $B_0 = 2 \times 10^{14}$ G and $\chi \sim 100$ (dip-60)
or $\chi \sim 1$ (dip-6, rand)

GEOMETRY PLAYS A CRUCIAL ROLE !

EM LUMINOSITY

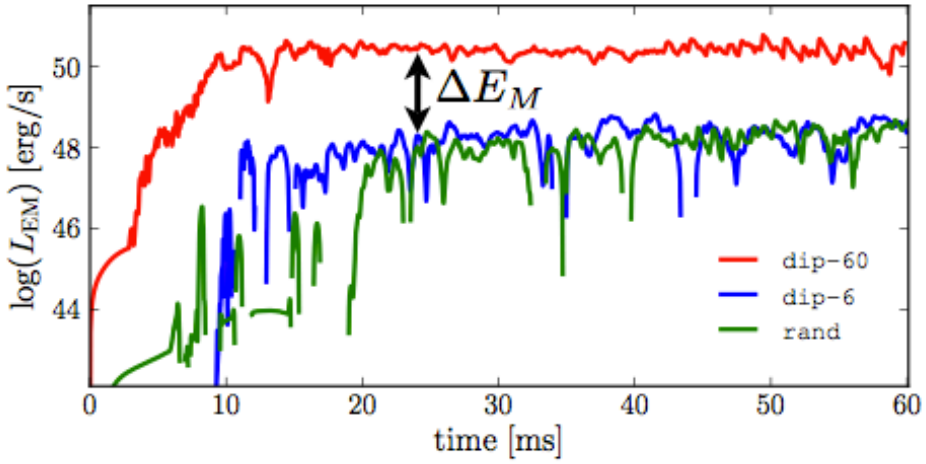

rescale energy in dip-60 to match dip-6

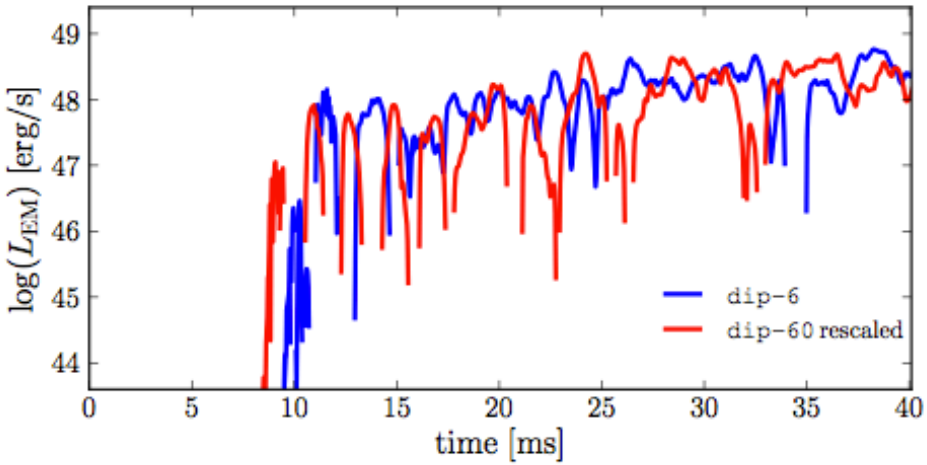

scale with initial magnetic energy

$$L_{\rm EM} \simeq 10^{48} \left(\frac{E_{\rm M}}{10^{44}\,{\rm erg}}\right)\left(\frac{R_e}{10^{6}\,{\rm cm}}\right)^{3}\left(\frac{P}{10^{-4}\,{\rm s}}\right)^{-1} {\rm erg\,s^{-1}}$$

where for the 3 geometries

$$E_{\rm M} \simeq (530,\ 1.5,\ 5.1) \times 10^{44}\,{\rm erg}$$

in terms of magnetic field strength at stationary stage:

$$L_{\rm EM} \simeq 10^{48} \left(\frac{\bar{B}}{10^{15}\,{\rm G}}\right)^{2}\left(\frac{R_e}{10^{6}\,{\rm cm}}\right)^{3}\left(\frac{P}{10^{-4}\,{\rm s}}\right)^{-1} {\rm erg\,s^{-1}}$$

these relations are 'universal'
(hold for different geometries)

CONNECTION TO SGRB OBSERVATIONS

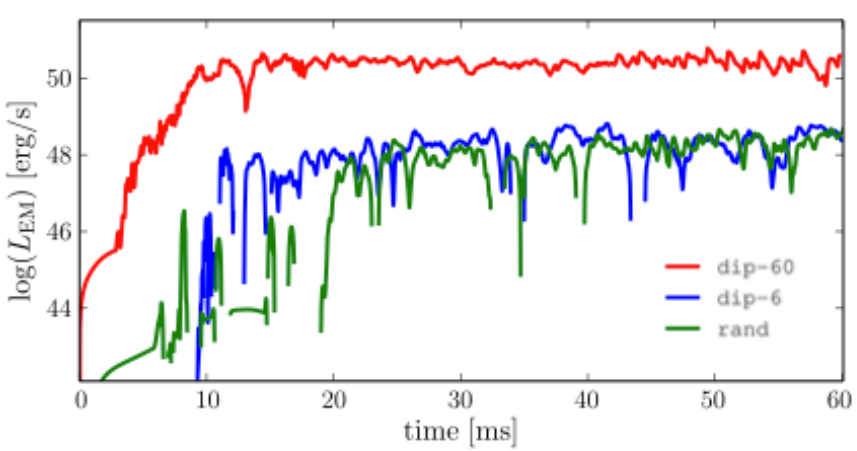

?

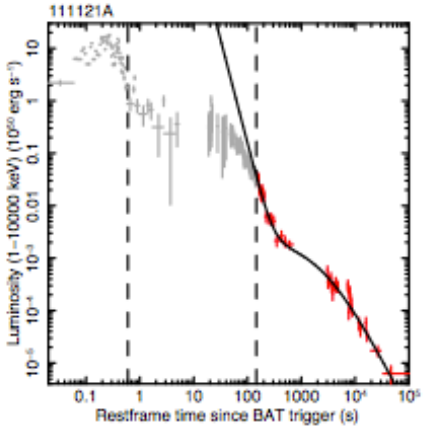

efficiency $\eta \equiv L_{\rm EM}^{\rm obs}/L_{\rm EM} \longrightarrow \eta \sim 0.01 - 0.1$

observed luminosity range $L_{\rm EM}^{\rm obs} \sim 10^{46} - 10^{51}\,{\rm erg\,s^{-1}}$ requires

MF strengths of $\bar{B} \sim 10^{14} - 10^{17}\,{\rm G}$

can be produced from progenitor strengths $\lesssim 10^{12}\,{\rm G}$ via

DURING MERGER

- compression of stellar cores
- Kelvin-Helmholtz instability

Zrake & MacFadyen 2013

IN THE POST-MERGER

- magnetic winding
- magneto-rotational instability

Siegel, Ciolfi, Harte & Rezzolla 2013 (see poster)

CONNECTION TO SGRB OBSERVATIONS

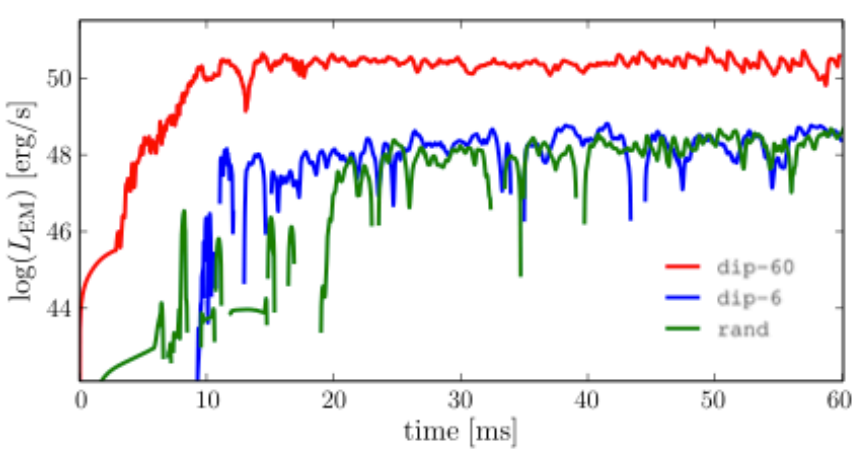

?

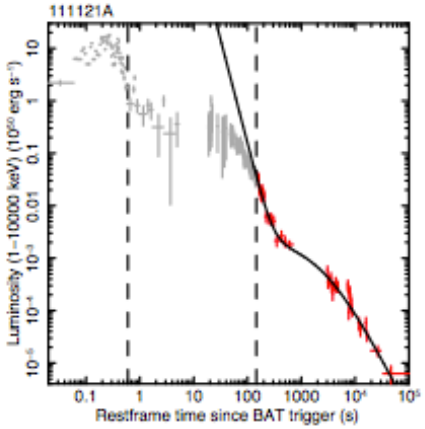

- GW PHASE : angular momentum removal by GWs within $\lesssim 1$ s ⟶ axisymmetry (if not, collapse to BH)

- DIFFERENTIAL ROTATION PHASE : lasts $\lesssim 10 - 100$ s for longer afterglows ↓

  1 - HMNS migrates to SMNS through substantial mass ejection

  2 - merger product is a SMNS ⟶ analogous evolution and emission mechanism
  (or a stable NS)

- PULSAR PHASE : diff. rotation is damped ⟶ transition to dipole spindown (t^{-2} decay observed in the longest X-ray plateaus)

SUMMARY

- long-lasting X-ray afterglows of SGRBs challenge the BH-torus leading scenario, suggesting the formation of a long-lived NS as outcome of BNS mergers
- magnetar model can explain the longer afterglows as dipole spindown, but not the early emission (prompt SGBR and so-called 'extended emission')
- we explore the early post-merger dynamics via 3D GRMHD simulations, starting from HMNS initial models
- robust feature of early evolution: baryon-loaded wind driven by diff. rotation
  - mostly isotropic, impact of MF geometry
  - substantial mass loss
  - high luminosites, compatible with observed X-ray afterglows
  - can explain long afterglows if combined with dipole spindown at later times, not enough to explain prompt SGRB emission

FUTURE DIRECTIONS: 1 - full BNS merger simulations
2 - lightcurve and spectrum

BACKUP SLIDES

INITIAL DATA

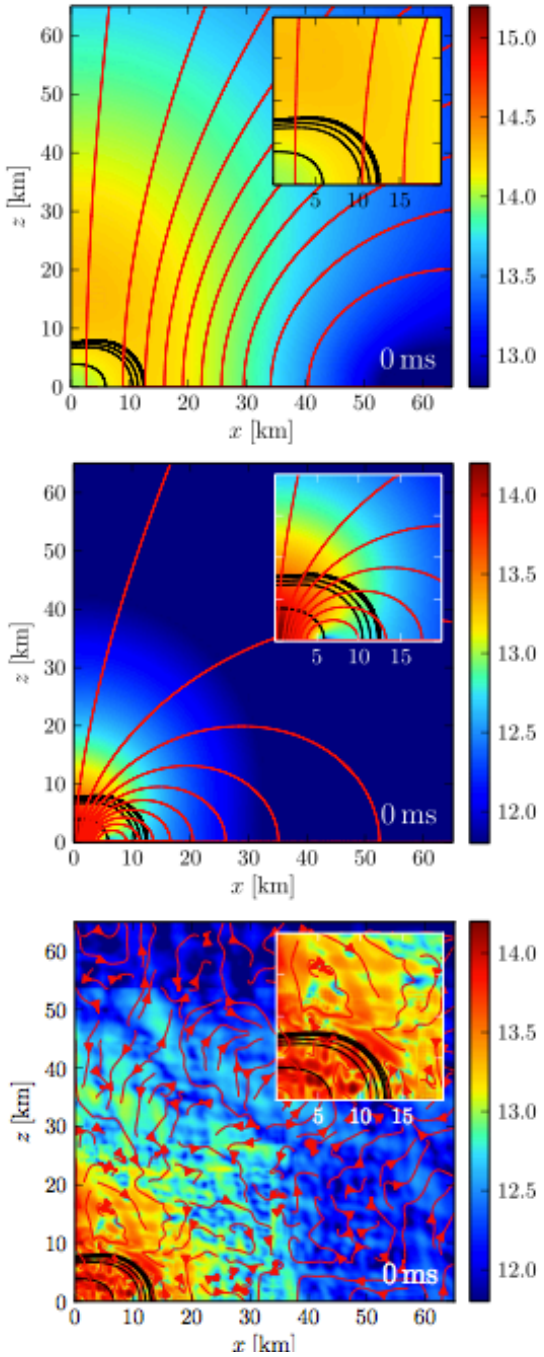

HMNS MODEL

$$M = 2.43\ \mathrm{M}_\odot$$

$$R_e = 11.2\ \mathrm{km}$$

DIFFERENTIAL ROTATION ⟵ $P_c = 0.47\ \mathrm{ms}$

j-constant law

$$A/R_e = 1.112$$

ideal fluid EOS

$$\Gamma = 2$$

Shibata et al. 2011
Kiuchi et al 2012

3 magnetic field geometries:

1 - DIPOLE 60 $\quad \varpi_{0,d} = 60\ \mathrm{km},\ 6\ \mathrm{km}$

2 - DIPOLE 6 $\quad A_\phi = A_{0,d}\varpi^2/(r^2+\varpi_{0,d}^2/2)^{3/2}$

3 - RANDOM

$$\boldsymbol{A}_{ijk} = \frac{A_{0,r}\sqrt{\gamma}}{(r^2+\varpi_{0,r}^2)^{3/2}} \sum_{\ell mn=0}^{n_k} \boldsymbol{a}_{\ell mn}\cos\left(\boldsymbol{x}_{ijk}\cdot\boldsymbol{k}_{\ell mn}+2\pi\boldsymbol{b}_{\ell mn}\right) + \boldsymbol{c}_{\ell mn}\sin\left(\boldsymbol{x}_{ijk}\cdot\boldsymbol{k}_{\ell mn}+2\pi\boldsymbol{d}_{\ell mn}\right)$$

superposition of ~ 6 x 10^4 modes with random amplitudes

maximum field strength 2×10^{14} G

initial magnetic energy $E_{\mathrm{M}} \simeq (530,\ 1.5,\ 5.1)\times10^{44}$ erg

MAGNETIC / FLUID PRESSURE RATIO

initial ratio $p_B/p_F \ll 10^{-5}$

at later times $p_B/p_F < 10^{-2} - 10^{-1}$

initial magnetic field represents a small perturbation to the stellar structure

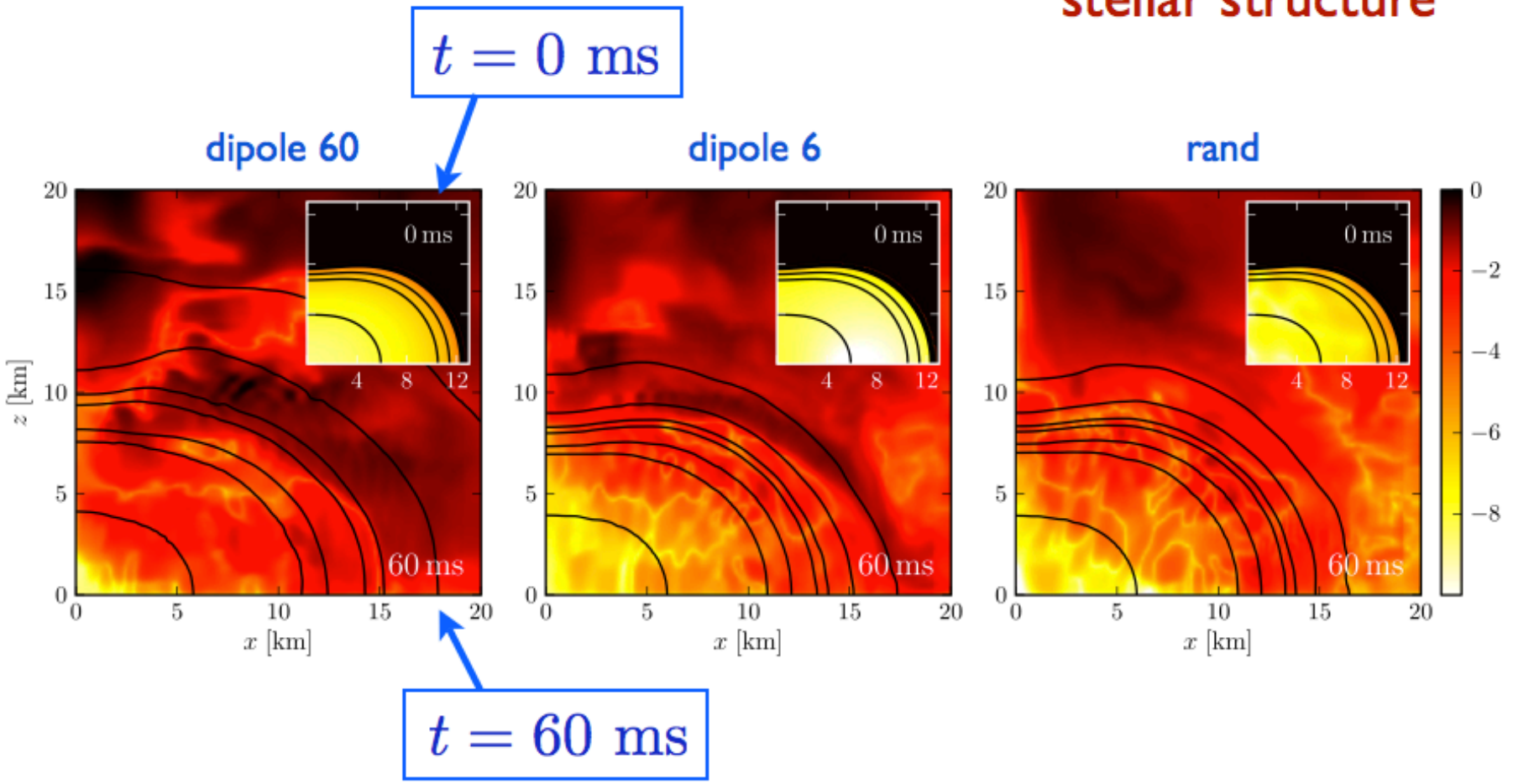

NUMERICAL SETUP

- cartesian grid: 7 ref levels, up to 1180 km, with finest resolution covering the star
- smallest grid spacing $h \approx 140$ m
- $\pi/2$ symmetry and z-reflection symmetry
- low-density atmosphere $\rho_{\rm atm} \simeq 6 \times 10^{-9} \rho_{\rm c}$

evolution performed with the Cactus Computational Toolkit and the WhiskyMHD code

Giacomazzo & Rezzolla 2007

ideal MHD, vector potential formulation, Lorentz gauge

(as in Giacomazzo & Perna 2013)

EM LUMINOSITY

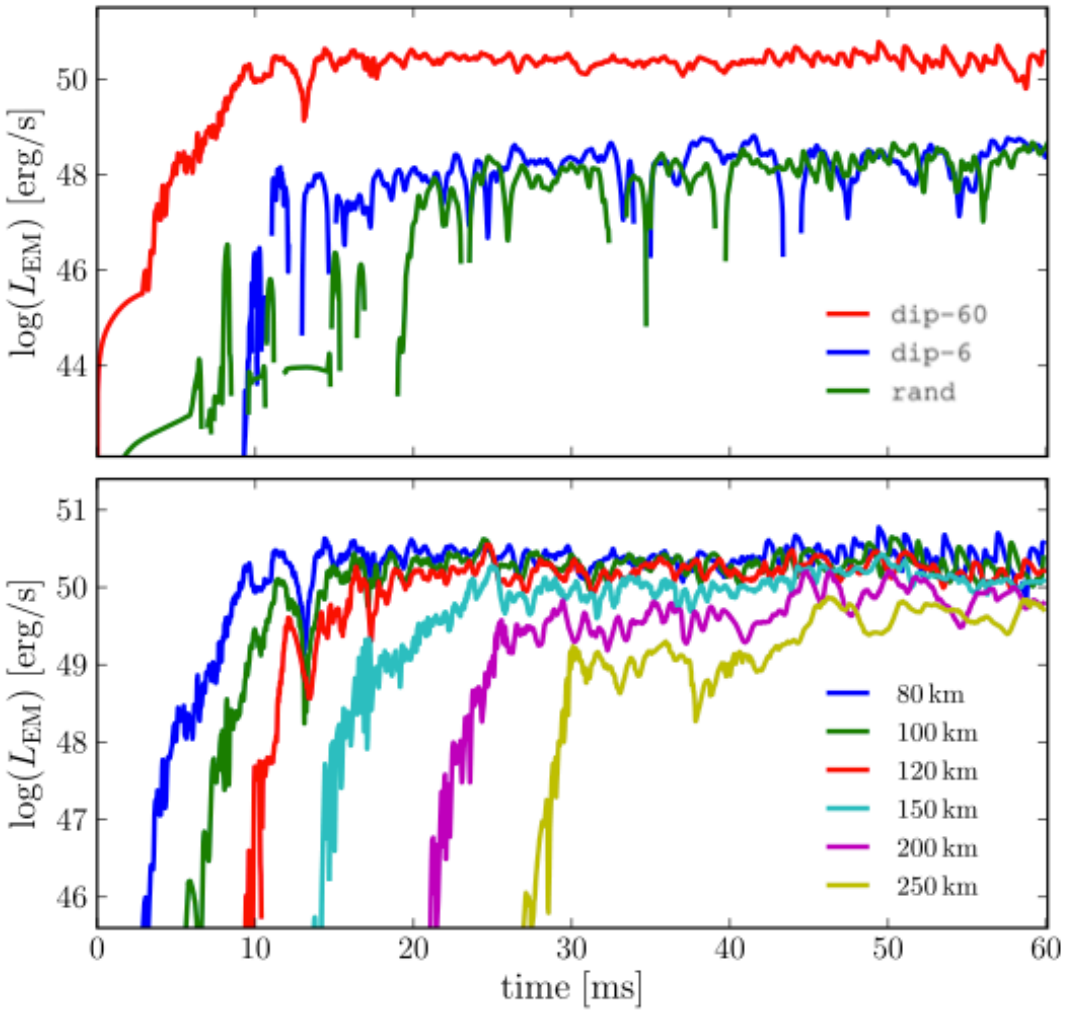

$$L_{\rm EM} \equiv -\oint_{r=R_{\rm d}} d\Omega \sqrt{-g}\,(T^{\rm EM})^{r}{}_{t}$$

$$\sim 10^{48} - 10^{50}\,{\rm erg\,s^{-1}}$$

EM LUMINOSITY - TESTS

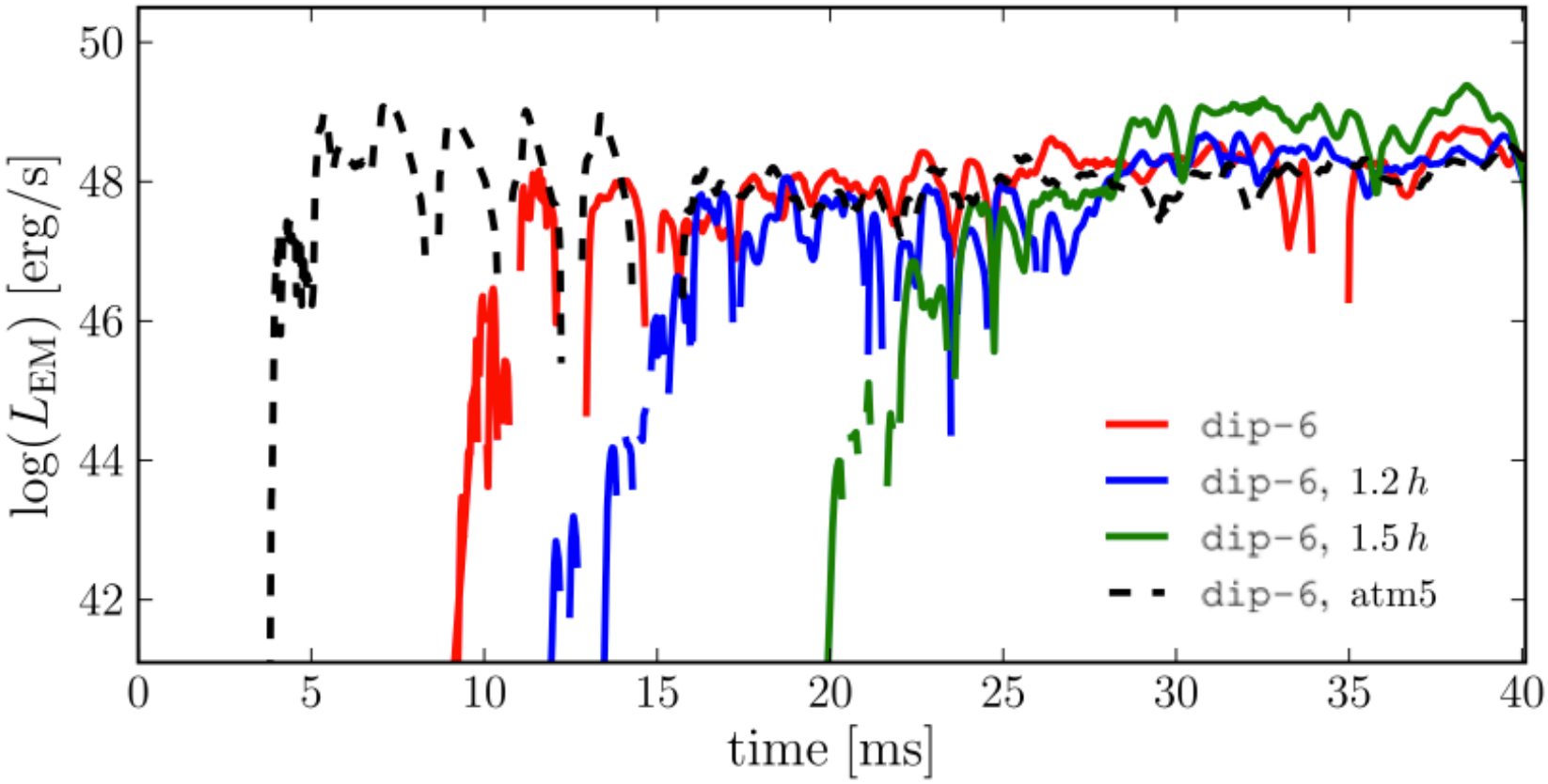

MHD EFFECTS: WINDING AND MRI

here we focus on the HMNS evolution prior to its collapse

two processes amplify the magnetic field and redistribute angular momentum:

- magnetic winding

poloidal magnetic field lines are wound up producing a toroidal component ;
in the linear regime toroidal fields are given by

$$B_{\rm tor} \approx (\varpi B^i \partial_i \Omega) t = a_{\rm w} t$$

- magneto-rotational-instability (MRI)

local linear instability of magnetized differentially rotating fluids ;
newtonian prediction for the fastest growing mode gives

$$\tau_{\rm MRI} \sim \Omega^{-1} \qquad \lambda_{\rm MRI} \sim \left(\frac{2\pi e^i_k}{\Omega}\right)\left(\frac{B_i}{\sqrt{4\pi\rho}}\right)$$

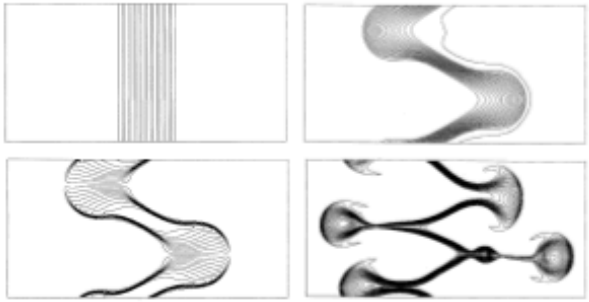

Hawley & Balbus 1991

HMNS EVOLUTION

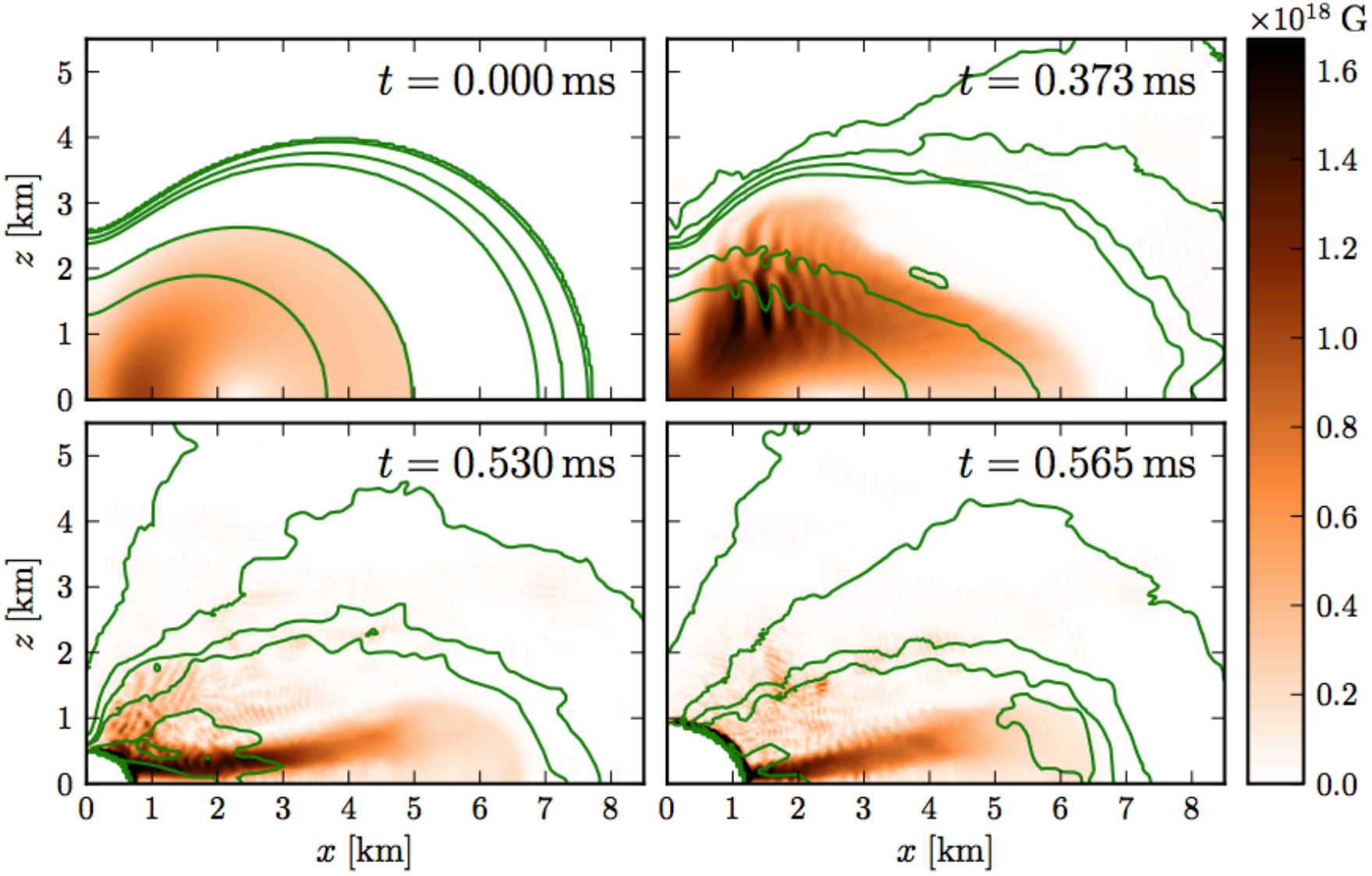

MAGNETIC FIELD AMPLIFICATION

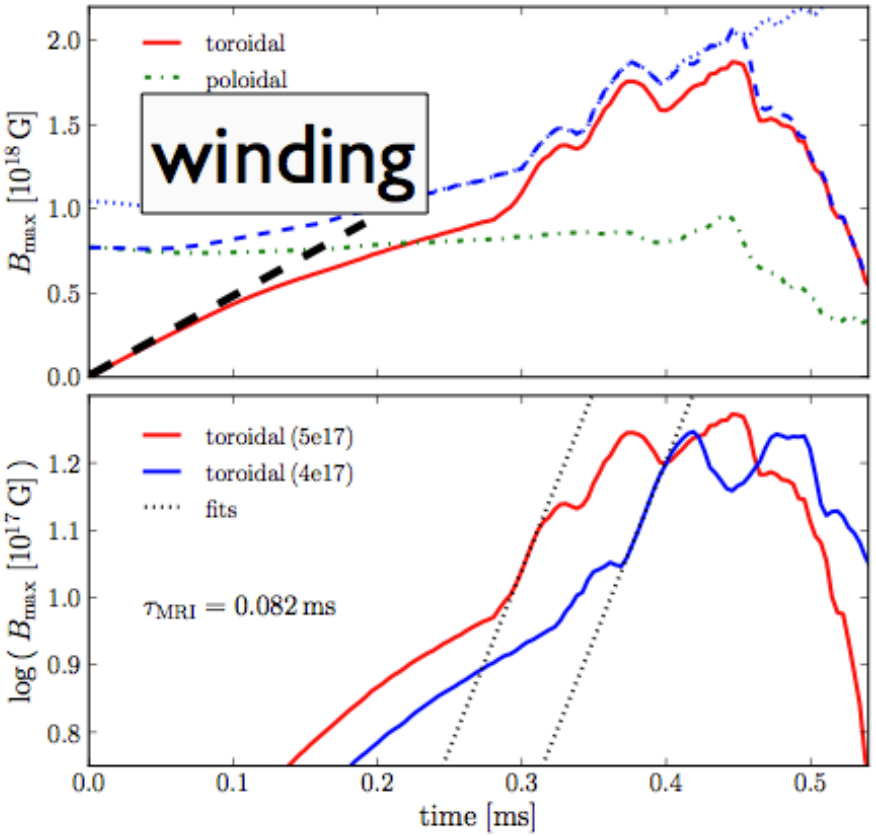

- poloidal field is not amplified during the evolution!
- toroidal field is produced at first by magnetic winding

$$B_{\mathrm{tor}} \approx a_{\mathrm{w}} t$$

MAGNETIC FIELD AMPLIFICATION

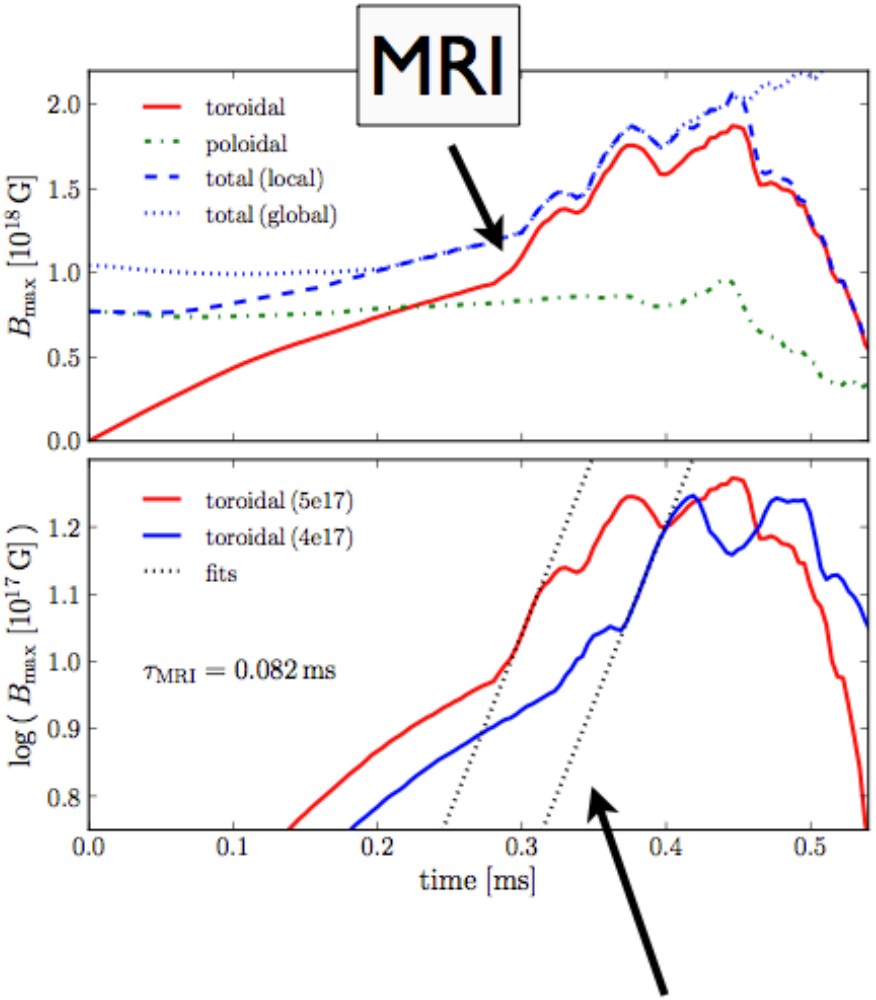

τ_{MRI} does not depend on magnetic field strength

- poloidal field is not amplified during the evolution!
- toroidal field is produced at first by magnetic winding

$$B_{\rm tor} \approx a_{\rm w} t$$

- then, MRI sets in!

the growth time is:

measure

$$\tau_{\rm MRI,fit} = (8.2 \pm 0.3) \times 10^{-2}\,{\rm ms}$$

vs

order-of-mag. prediction

$$1/\Omega \approx (4-5) \times 10^{-2}\,{\rm ms}$$

MRI vs RESOLUTION and MF STRENGTH

$$\lambda_{MRI} \propto B$$

- different resolutions at fixed magnetic field

$$B_c^{\rm in} = 5 \times 10^{17}\ {\rm G}$$

- different magnetic field strengths at fixed resolution (h)

$$B_c^{\rm in} = (1, 3, 4, 5) \times 10^{17}\ {\rm G}$$

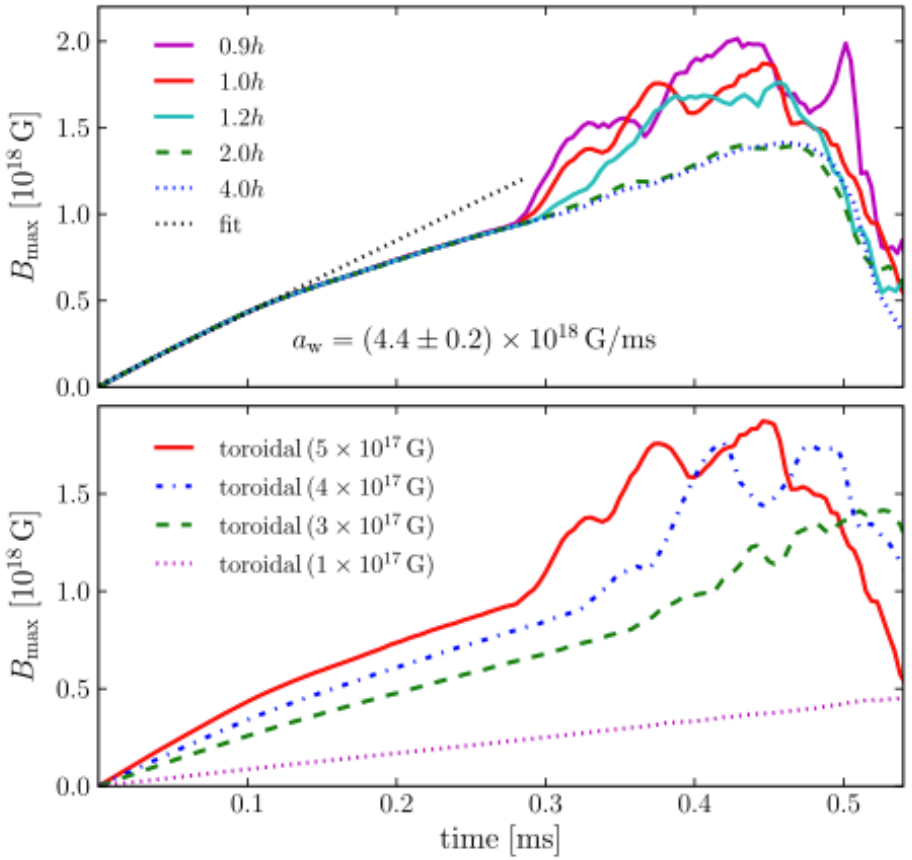

MRI disappears by lowering B or the resolution, while magnetic winding is always as predicted

MRI WAVELENGTH

- power spectrum reveals one single mode $k_{\rm MRI}$ (plus contributions from gradients over the selected region)
- it corresponds to

$$\lambda_{\rm MRI} \sim 0.4 \text{ km}$$

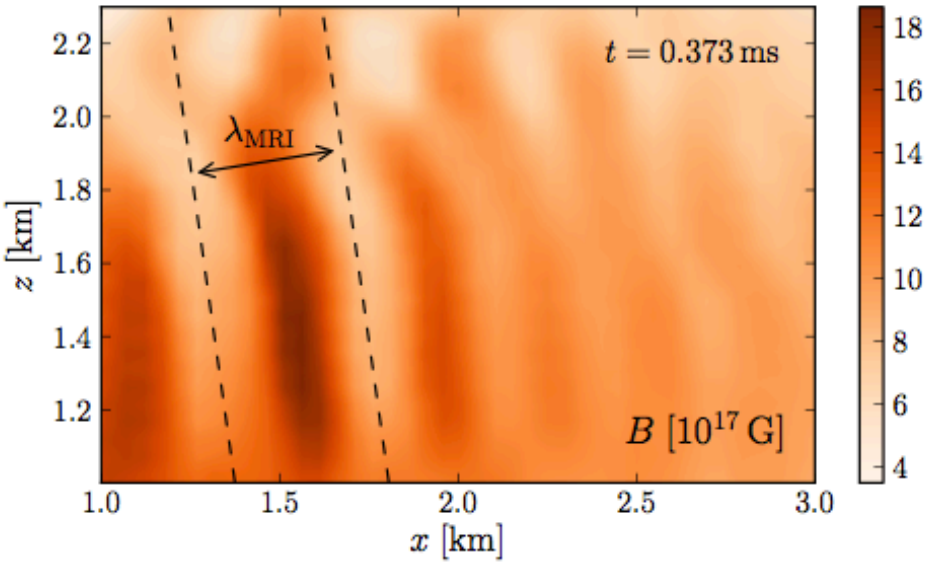

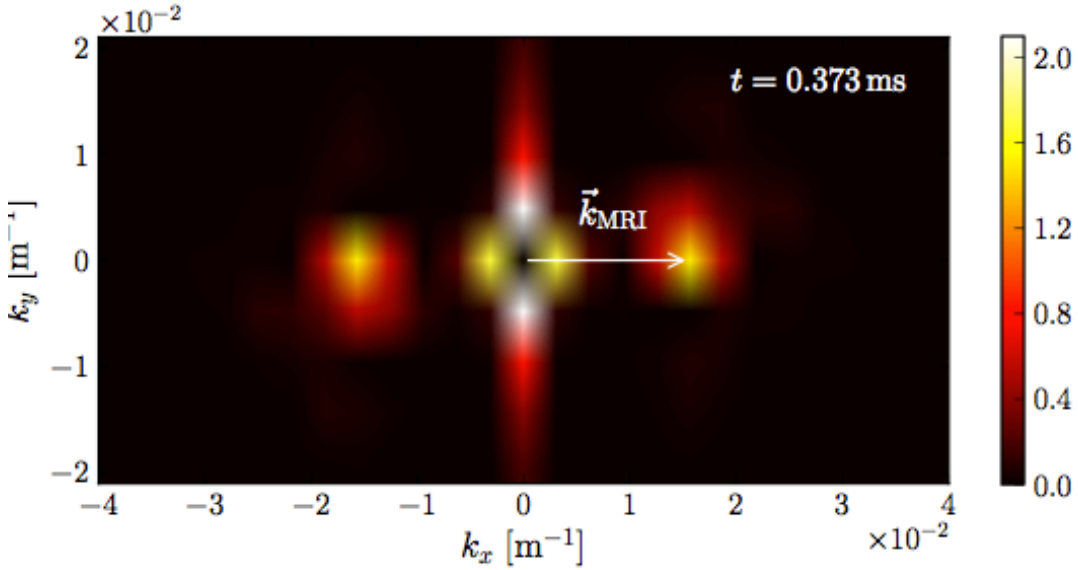

~0.4 km consistent with the strongest channel flows

ripples are also tilted by

$$\theta_{kx} \approx 3^\circ - 7^\circ$$

match with order-of-magnitude theoretical prediction

$$\lambda_{\rm MRI,theo} \approx (0.5 - 1.5) \text{ km}$$